Supplementary Information

Monitoring The Synthesis of Neutral Lipids in Lipid Droplets of Living Human Cancer Cells using Two-color Infrared Photothermal Microscopy

Chanjong Park,[1,2] Jong Min Lim,[1,†] Seok-Cheol Hong,[1,3] and Minhaeng Cho[1,2]

[1]*Center for Molecular Spectroscopy and Dynamics, Institute for Basic Science, Seoul, 02841 Korea.*

[2]*Department of Chemistry, Korea University, Seoul, 02841 Korea.*

[3]*Department of Physics, Korea University, Seoul, 02841 Korea.*

[†]Present address: *Department of Chemistry, Kyungpook National University, Daegu 41566, Korea.*

Table of Contents

Supplementary Note 1. Experimental setup of our two-color IR photothermal microscope

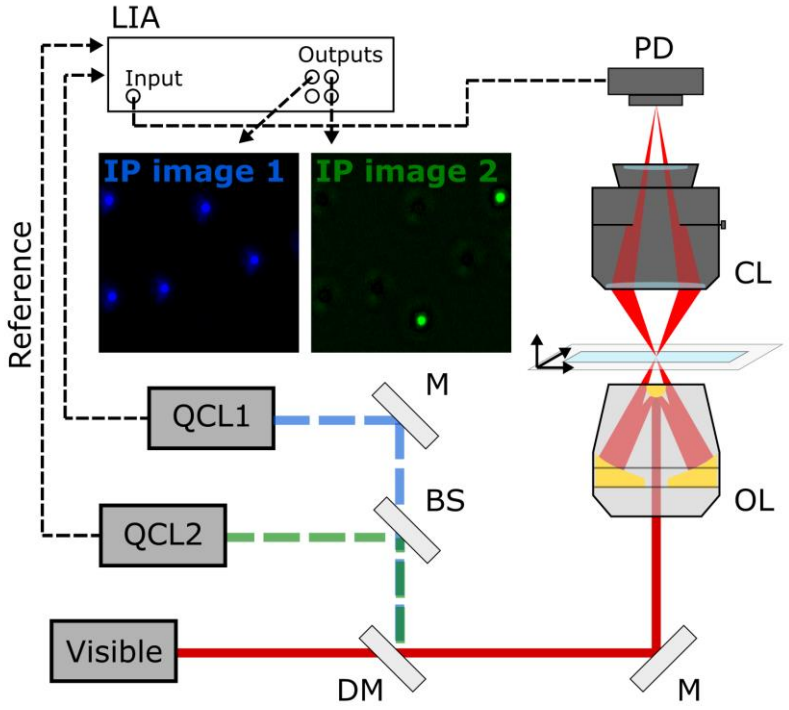

Figure S1. Illustration of two-color IPM setup. Instrumental configuration of two-color IP microscope. QCL, quantum cascade laser; M, mirror; BS, beamsplitter; OL, objective lens; CL, condenser lens; PD, photodiode; LIA, lock-in amplifier.

Two IR excitation pulses from two QCLs (Daylight Solutions, 31049-HHG and 31035-HHG-UT, 1,980 cm^{-1} to 2,239 cm^{-1} and 2,740 cm^{-1} to 2,970 cm^{-1}, respectively) and a 640 nm CW probe beam from a DPSS laser (LASOS, RLK 40100 TS) are employed to generate two independent IPI contrasts and measure them, respectively. Those three beams are combined coaxially by a 50:50 CaF_2 beamsplitter (Thorlabs, BSW510) and a dichroic mirror (ISP Optics, BSP-DI-25-2). The spatially overlapped laser beams are focused onto a specimen by a high NA reflective objective lens (Horiba, 0.66 NA, UVI 74x). At the focus, each IR excitation pulse train excites a specific molecular vibration and induces a time-dependent refractive-index gradient (also called a thermal lens), modulating the physical properties, such as scattering and divergence, of the co-propagating visible probe beam at the repetition rate of each IR excitation pulse. The probe beam in the transmission is collected by a variable aperture condenser and directed to a silicon-amplified detector (Thorlabs, PDA36A-EC). Notably, there is an iris diaphragm inside the condenser, which is adjusted to maximize the intensity modulation of the probe beam by constructing a dark-field-like geometry. The detector output is sent to the lock-in amplifier (Zurich instruments, HF2LI), which has two oscillators for setting up lock-in

frequency and six different demodulators for signal processing. Two demodulators referenced to the repetition rates of two QCLs selectively measure each IR-resonant photothermal signal from the multiplexed IR photothermal signals, which are then delivered to a data acquisition (DAQ) device (National Instruments, PCIe-6361). A custom-built code is used to construct the IR photothermal images, controlling a piezo scanner (PI, P-545.3C8H) for sample scanning and the data acquisition process with the DAQ device. The scanner is equipped with a miniaturized incubation system for long-term live-cell imaging, which maintains CO_2 concentration, humidity, and temperature.

Supplementary Note 2. IP spectra of palmitic acid-d_{31} solutions in ethanol

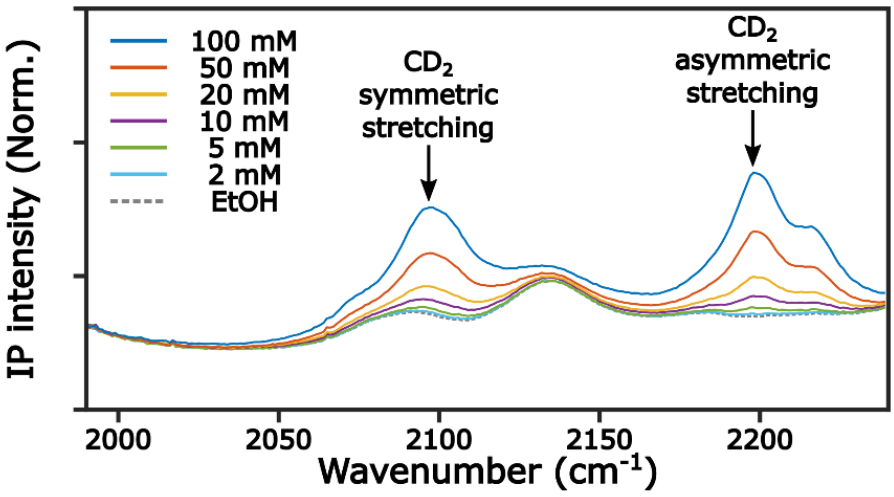

Figure S2. IP spectra of palmitic acid-d_{31} solutions with different concentrations. Each data point in the IP spectra was obtained by 50-ms averaging and normalization to the intensity of the IR excitation pulse. Step size, 1 cm^{-1}. To clearly show the concentration dependence of IP signals, IP intensities at two specific wavelengths (2,096 cm^{-1} and 2,193 cm^{-1}), corresponding to CD_2 symmetric and asymmetric stretching vibrations, respectively, were plotted with respect to the concentration of PA-d_{31} solution in Figure 1E.

Supplementary Note 3. Background IP signal from water

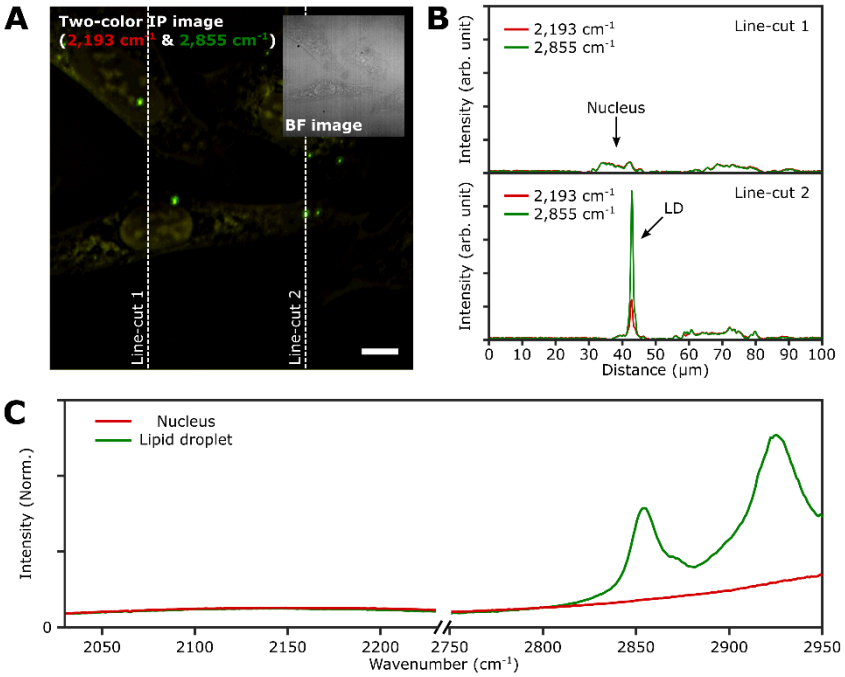

Figure S3. Matching background signal in two-color IPI measurement. (**A**) Two-color IP image of U2OS cells. The green and red false colors indicate IPI contrasts of 2,855 cm^{-1} and 2,193 cm^{-1}, respectively. Cutoff frequency, 70 Hz. Step size, 200 nm. Pixel dwell time, 2 ms. Probe power, 15 mW. IR excitation power, 0.2 mW (at 2,193 cm^{-1}) and 0.1 mW (at 2,855 cm^{-1}). Scale bars, 10 μm. (**B**) Comparison of line-cut profiles in two-color IP images. Red and green lines represent the IP intensities of 2,193 cm^{-1} and 2,855 cm^{-1}, respectively, and the top and bottom plots correspond to the signals acquired along the white dotted line cuts 1 and 2 in Figure S3A. (**C**) IP spectra of nucleus and LD. Each data point in the IP spectra was obtained by 50-ms averaging and normalization to the intensity of the IR excitation pulse. Step size, 1 cm^{-1}.

As noted in the main text, the IR absorption of background water affects IPI contrasts. Although it is hard to remove the unwanted effect in IP signals selectively, this effect could be addressed by matching the background IP signals measured in our two-color IPI technique. Figure S3A is the two-color IP image of normal U2OS cells with IR excitations of 2,193 cm^{-1} (50 kHz) and 2,855 cm^{-1} (45 kHz), where the background water signals of two IPI contrasts were matched by tuning the powers of IR excitations. The inset in the top right shows the corresponding bright-field image. We were able to observe several round-shaped organelles that respond strongly to 2,855 cm^{-1} of IR excitation (colored in green), assumed to be LDs. Although other cellular structures (particularly the nucleus) were also vaguely identified in the

IP image, their IP intensities at 2,193 cm^{-1} and 2,855 cm^{-1} were the same as shown in Figure S3B. The IPI contrasts with the same intensities at two different IR wavelengths originated from the IR absorption of water, only amplified due to the stronger scattering environment of intracellular organelles. The IP spectra obtained from the nucleus and LD clearly show that our IPI measurement could not detect any IR absorption peaks related to CH vibrations in the nucleus, unlike in the LD (Figure S3C).

Supplementary Note 4. Calibration of the IP spectra

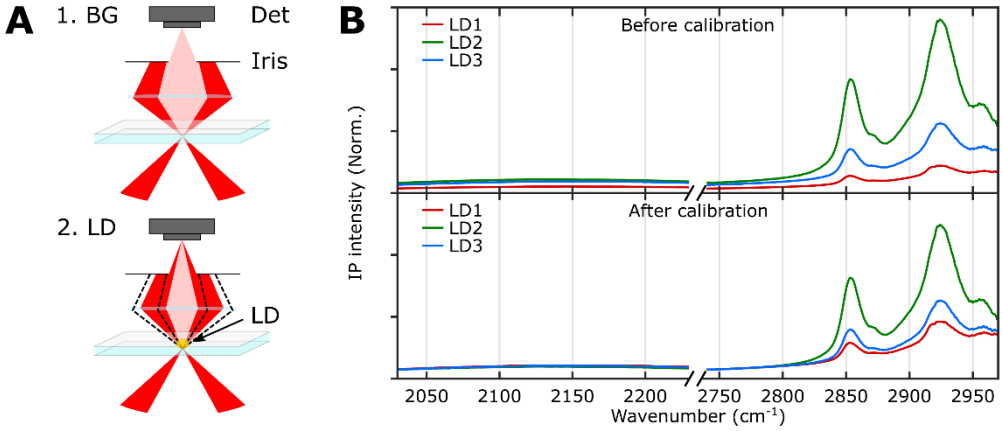

Figure S4. Calibration of IP spectra in investigating LDs. (**A**) Illustration of probe beam in the detection beam path. The top and bottom images depict the detection beam path when the probe beam's focus is positioned at the background water and the LD, respectively. The black dotted lines in the bottom image represent the original beam path of ballistic photons. Det; detector. (**B**) Full range IP spectra of LDs before and after background calibration. Three LDs are indicated in Figure 2A. Each data point in the IP spectra was obtained by 50-ms averaging and normalization to the intensity of the IR excitation pulse. The spectra on the bottom were calibrated by matching the background signal level in the off-resonant spectral region (2,740 cm^{-1} to 2,760 cm^{-1}). Stepsize, 1 cm^{-1}.

Our IPI system employs dark-field geometry, where the illumination and scattered photons are spatially separated in the detection path (Figure S4A, top). The majority of ballistic illumination photons were rejected by using an iris positioned before the detector, resulting in the dominance of scattering photons in the detected intensity of the probe beam. The detected intensity is proportional to the square of the incident probe field and scattering amplitude (Y. Bai *et al.*, *Sci. Adv.* 2021, **7**, eabg1559) as follows:

$$I_{det} \propto |E_{in}|^2 \times |s|^2, \qquad (S1)$$

where I_{det} is the detected intensity of the probe beam, E_{in} and s are the incident probe field and the scattering amplitude at the focus, respectively. It should be noted that the term "proportional" implies that the detected intensity can vary depending on the optical configuration and sample condition. For example, I_{det} could be perturbed in measuring different LDs due to their different sizes and shapes (Figure S4A, bottom), posing challenges in accurately measuring and comparing their IP signals. In order to ensure precise and reliable measurements, it is crucial to conduct a calibration process that aligns the IP signals over a background spectral region (2,740 cm^{-1} to 2,760 cm^{-1}). Note that the calibration constant

remains consistent across two distinct spectral regions in our two-color IPM (Figure S4B). As a result, regardless of the size and dimensions of the LDs, we are able to compare IP spectra measured from various LDs in the full spectral range (1,980 to 2,239 cm^{-1} and 2,740 to 2,970 cm^{-1}) without being affected by changes in the detected intensity of probe beam.

Supplementary Note 5. IP spectra of lipid droplets in U2OS cells

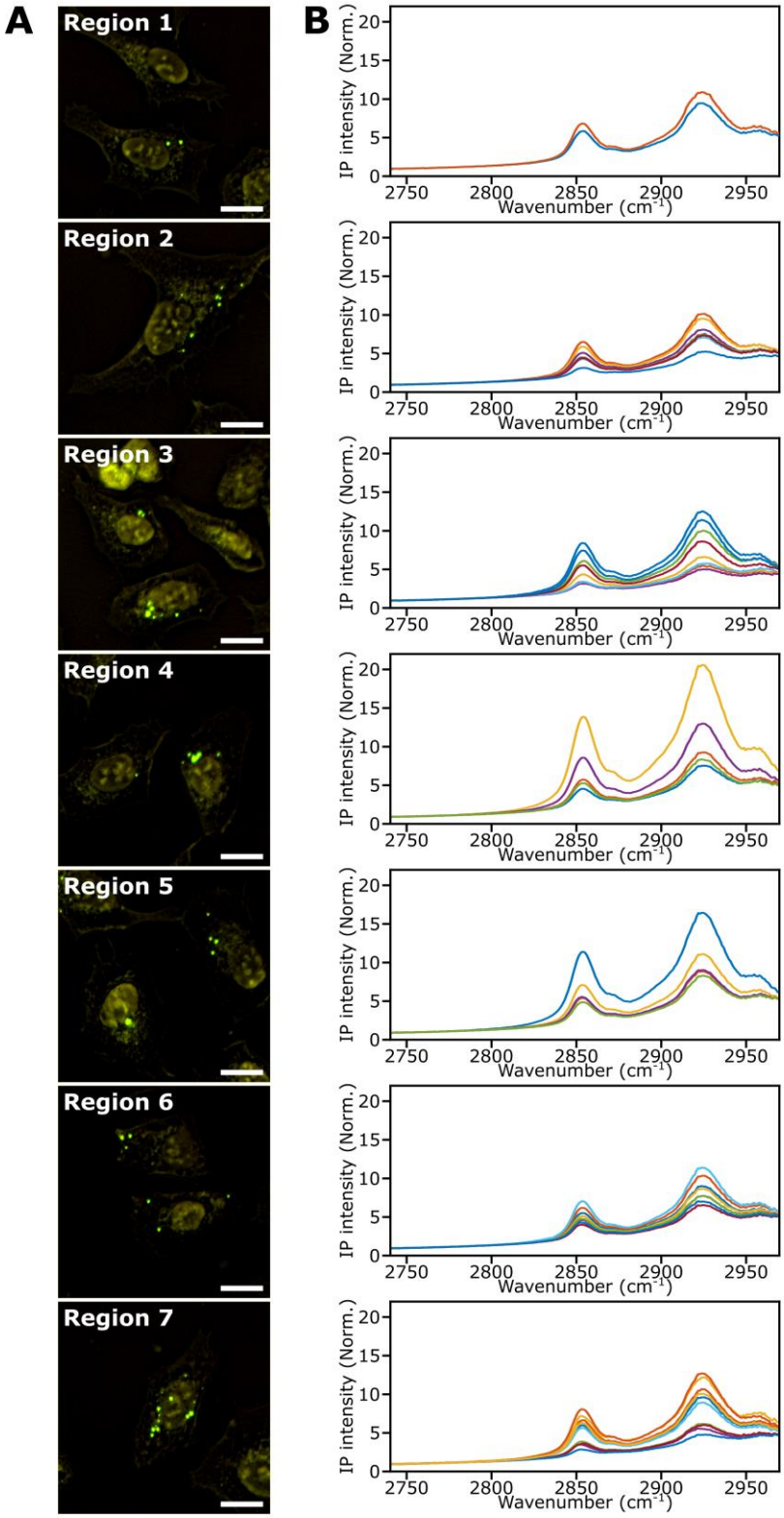

Figure S5. IP images and spectra of LDs analyzed in Figure 2C. (**A**) Two-color IP images of U2OS cells measured at 7 different regions. The color scheme is the same as in Figure S3A (red: 2,193 cm^{-1}, green: 2,855 cm^{-1}). Cutoff frequency, 70 Hz. Step size, 200 nm. Pixel dwell time, 2 ms. Probe power, 15 mW. IR excitation power, 0.2 mW (at 2,193 cm^{-1}) and 0.1 mW (at 2,855 cm^{-1}). Scale bars, 20 μm. (**B**) IP spectra of 47 LDs identified in Figure S5A. Each data point in the IP spectra was obtained by 50-ms averaging and normalization to the intensity of the IR excitation pulse. Step size, 1 cm^{-1}.

Supplementary Note 6. Comparative fluorescence imaging with Nile Red

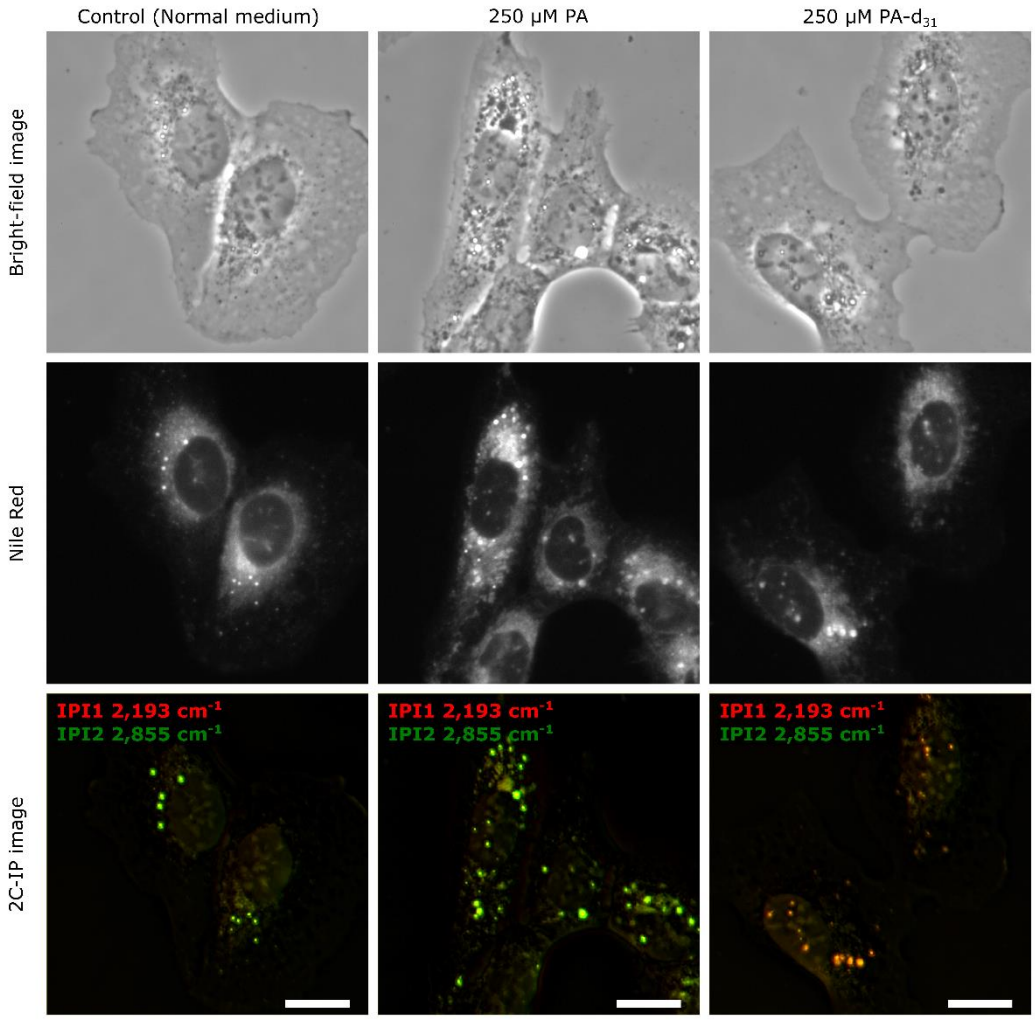

Figure S6. Comparative fluorescence imaging with Nile Red. Bright-field (top), fluorescence (middle), and two-color IP images (bottom) of fixed U2OS cells cultured in different growth media (250 μM PA, 250 μM PA-d_{31}, and standard medium) for 24 hours. The U2OS cells were stained with 500 nM Nile Red for 30 minutes before fluorescence imaging measurement. The color scheme of the 2C-IP image is the same as in Figure S3A (red: 2,193 cm^{-1}, green: 2,855 cm^{-1}). Cutoff frequency, 70 Hz. Step size, 200 nm. Pixel dwell time, 2 ms. Probe power, 15 mW. IR excitation power, 0.2 mW (at 2,193 cm^{-1}) and 0.1 mW (at 2,855 cm^{-1}). Scale bars, 20 μm.

Supplementary Note 7. Observation of neutral lipid synthesis in Huh-7 cell line

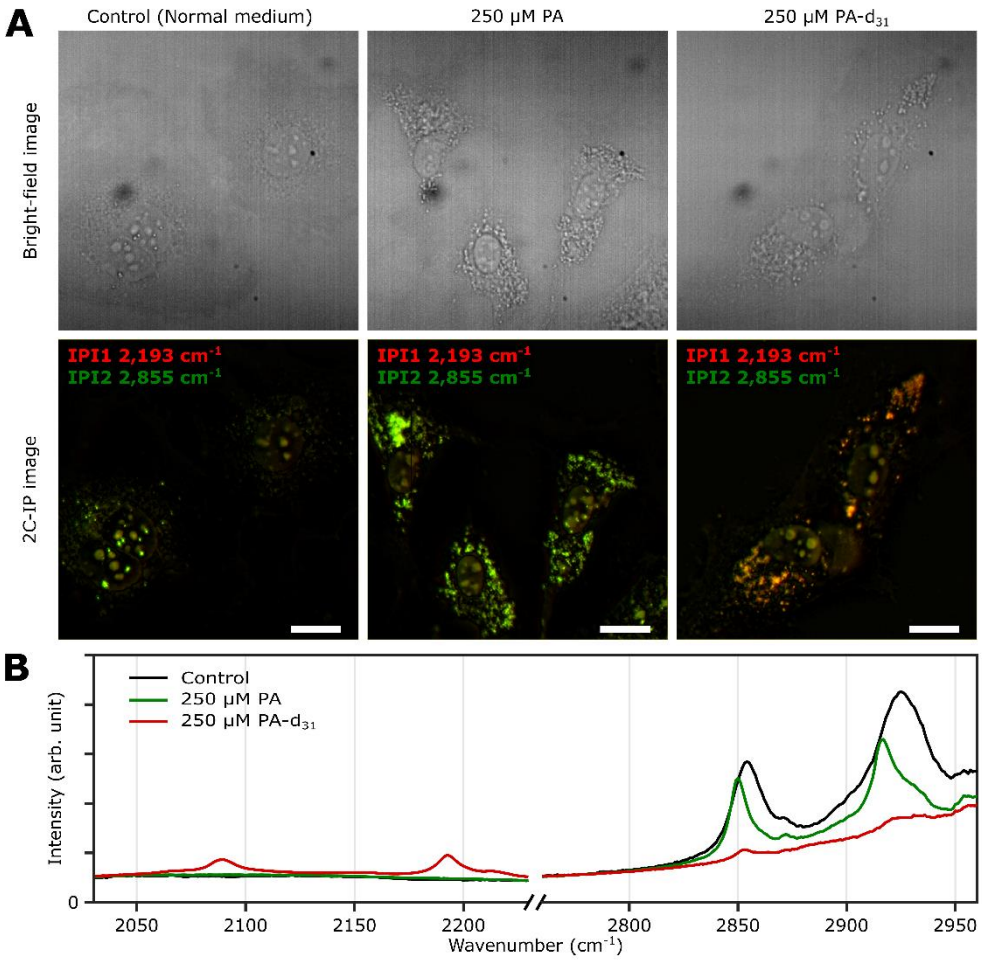

Figure S7. Observation of neutral lipid synthesis in Huh-7 cell line (**A**) Bright-field (top) and IP images (bottom) of fixed Huh-7 cells cultured in different growth media (250 μM PA, 250 μM PA-d_{31}, and standard medium) for 24 hours. The color scheme of the 2C-IP image is the same as in Figure S3A (red: 2,193 cm^{-1}, green: 2,855 cm^{-1}). Cutoff frequency, 70 Hz. Step size, 200 nm. Pixel dwell time, 2 ms. Probe power, 15 mW. IR excitation power, 0.2 mW (at 2,193 cm^{-1}) and 0.1 mW (at 2,855 cm^{-1}). Scale bars, 20 μm. (**B**) Representative IP spectra of LDs observed in Figure S7. Each data point in the IP spectra was obtained by 50-ms averaging and normalization to the intensity of IR excitation pulse. Step size, 1 cm^{-1}.

Supplementary Note 8. Calculation of the mole fractions of CH_2 and CD_2 lipid species from IP measurements

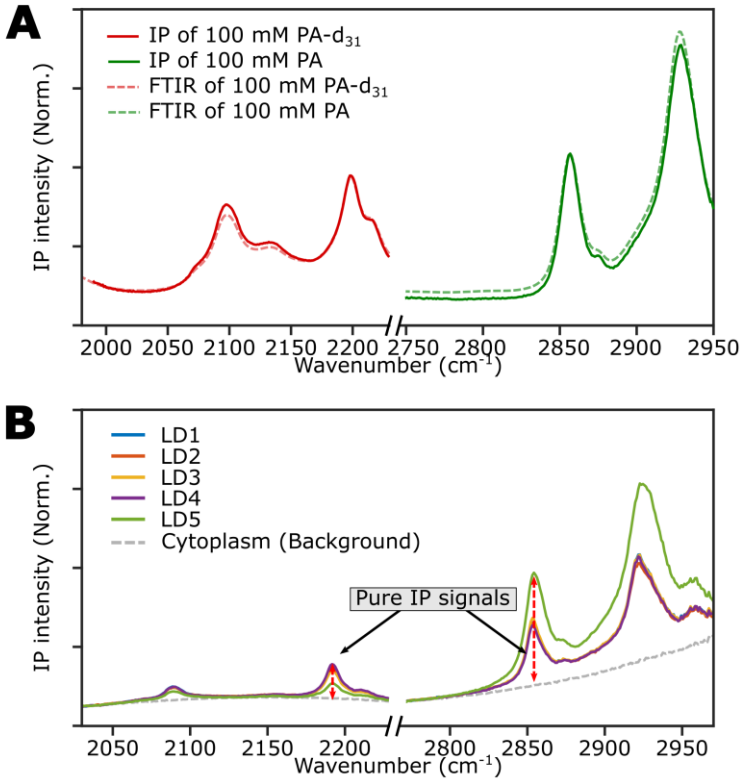

Figure S8. Calculation of the mole fractions in IP measurement (**A**) FT-IR and IP spectra of 100 mM PA and PA-d_{31} solutions. The solid and dashed lines represent the IP and FT-IR spectra, respectively. Each data point in the IP spectra was obtained by 50-ms averaging and normalization to the intensity of IR excitation pulse. Step size, 1 cm^{-1}. Both IP spectra in different IR windows were multiplied by the same constant to match the IP spectra with the corresponding FT-IR spectra. (**B**) Substraction of water background from IP spectra. Each data point in the IP spectra was obtained by 50-ms averaging and normalization to the intensity of IR excitation pulse. Step size, 1 cm^{-1}.

A. Derivation of the equation for calculating mole fractions

To calculate the mole fractions of newly synthesized lipids using the measured IP signal, we should first examine the meaning of the IP signal. Figure S8A shows the FT-IR and IP spectra of 100 mM solutions of PA and PA-d_{31} dissolved in ethanol-d_6 and ethanol, respectively, where both IP spectra were multiplied by the same constant to match their scales with FT-IR spectra. The spectral match between the IP spectrum and the FT-IR spectrum indicates that the IP signal at a specific wavelength (λ) is directly proportional to the IR absorbance of the sample. The requirement of the same constant for scaling both IP spectra suggests that the proportionality

constant remains consistent throughout the IP measurements. The IP signal, denoted as *S*, can thus be expressed as follows:

$$S(\lambda) = k\sigma_A(\lambda)C_A, \quad (S2)$$

where k is the proportionality constant, $\sigma_A(\lambda)$ is the absorption cross-section of molecule A at wavelength λ, and C_A is the molar concentration of A. As shown in Equation S1, due to the presence of the proportionality constant, directly determining the concentration of a molecule is challenging with the IP signal. However, calculating the mole fraction is relatively straightforward and enables comparisons between different molecules. If LDs are assumed to contain two types of lipids (CD_2 and CH_2) with perfectly distinguished absorption peaks at λ_1 and λ_2, respectively, the mole fraction (MF), χ, of CD_2 lipid species in LD can be obtained as follows

$$\chi_{CD_2} = \frac{C_{CD_2}}{C_{CD_2} + C_{CH_2}}. \quad (S3)$$

By multiplying the constants of $k, \sigma_{CD_2}(\lambda_1), and\ \sigma_{CH_2}(\lambda_2)$ to both the numerator and denominator of Equation S3, we obtain

$$\chi_{CD_2} = \frac{k \times \sigma_{CD_2}(\lambda_1) \times \sigma_{CH_2}(\lambda_2) \times C_{CD_2}}{k \times \sigma_{CD_2}(\lambda_1) \times \sigma_{CH_2}(\lambda_2) \times C_{CD_2} + k \times \sigma_{CD_2}(\lambda_1) \times \sigma_{CH_2}(\lambda_2) \times C_{CH_2}}. \quad (S4)$$

According to Equation S2, the mole fraction of CD_2 lipids can be expressed as follows:

$$\chi_{CD_2} = \frac{\sigma_{CH_2}(\lambda_2)S_{CD_2}(\lambda_1)}{\sigma_{CH_2}(\lambda_2)S_{CD_2}(\lambda_1) + \sigma_{CD_2}(\lambda_1)S_{CH_2}(\lambda_2)}. \quad (S5)$$

Therefore, we could calculate the mole fractions of newly synthesized lipid species within LDs by only using the IP signals and their IR absorption cross-sections at the two specific wavelengths corresponding to CD_2 and CH_2.

B. Calculation of mole fractions with measured IP spectra

In the following section, we will elucidate the procedure for calculating mole fractions utilizing the derived equation and measured IP spectra. As shown in Equation S5, this procedure requires four fundamental values: the IP signals corresponding to CD_2 and CH_2 and their respective absorption cross-sections. For the sake of computational simplicity, the absorption cross-section values were substituted with the IR absorbance values of PA-d_{31} and PA of Figure 1C in the present demonstration. Note that the IP signal includes background signal originating from water, necessitating their exclusion for precise calculation of mole fractions as mentioned in Supplementary Information 3. To address this, we obtained the IP spectra from the cell cytoplasm to serve as background spectra, which were subsequently subtracted from the IP spectra obtained from LDs (Figure S8B), where the IP spectra of LDs provided as an example are the ones utilized in Figure 4C. Through this approach, we were

able to isolate the pure IP signals corresponding to CD_2 and CH_2 lipids from individual LDs, effectively eliminating the influence of water-induced background signals. Utilizing these refined values, we calculated the mole fractions of CD_2 and CH_2 lipids within each LD.

Supplementary Note 9. Distribution of CD_2 and CH_2 molecule fractions in each lipid droplet

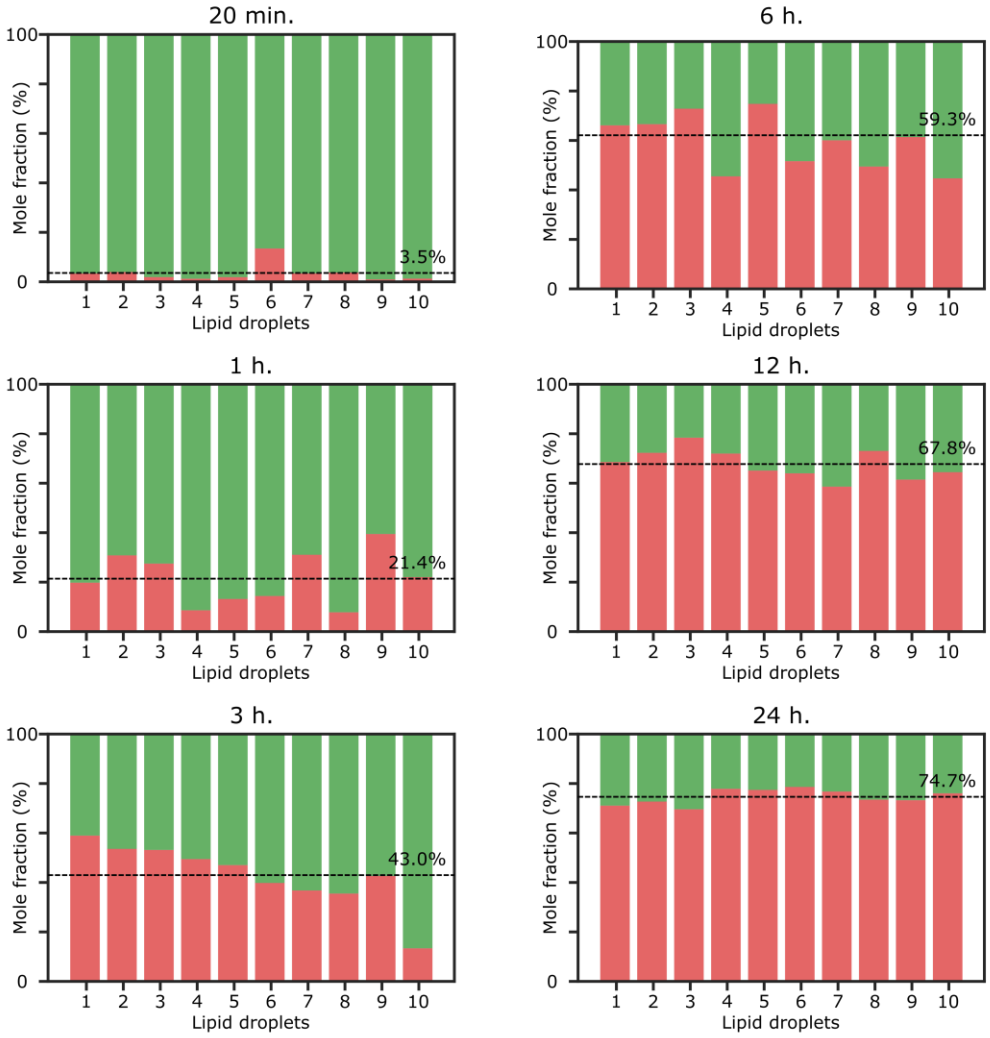

Figure S9. Calculation of mole fractions in each lipid droplet used in Figure 4D. Two wavelengths of 2,193 cm^{-1} and 2,855 cm^{-1} were chosen for both the measurement of IP spectra and calculation of mole fractions. The exposure time of U2OS cells to PA-d_{31} is indicated at the top of each graph. The red and green columns represent the mole fractions of lipids containing CD_2 and CH_2 chemical bonds, respectively. The black dashed lines are the average mole fraction of CD_2 lipid species at each treatment time.

Supplementary Note 10. Time-lapse 2C-IP images of living U2OS cells exposed to 250 µM palmitic acid-d_{31}

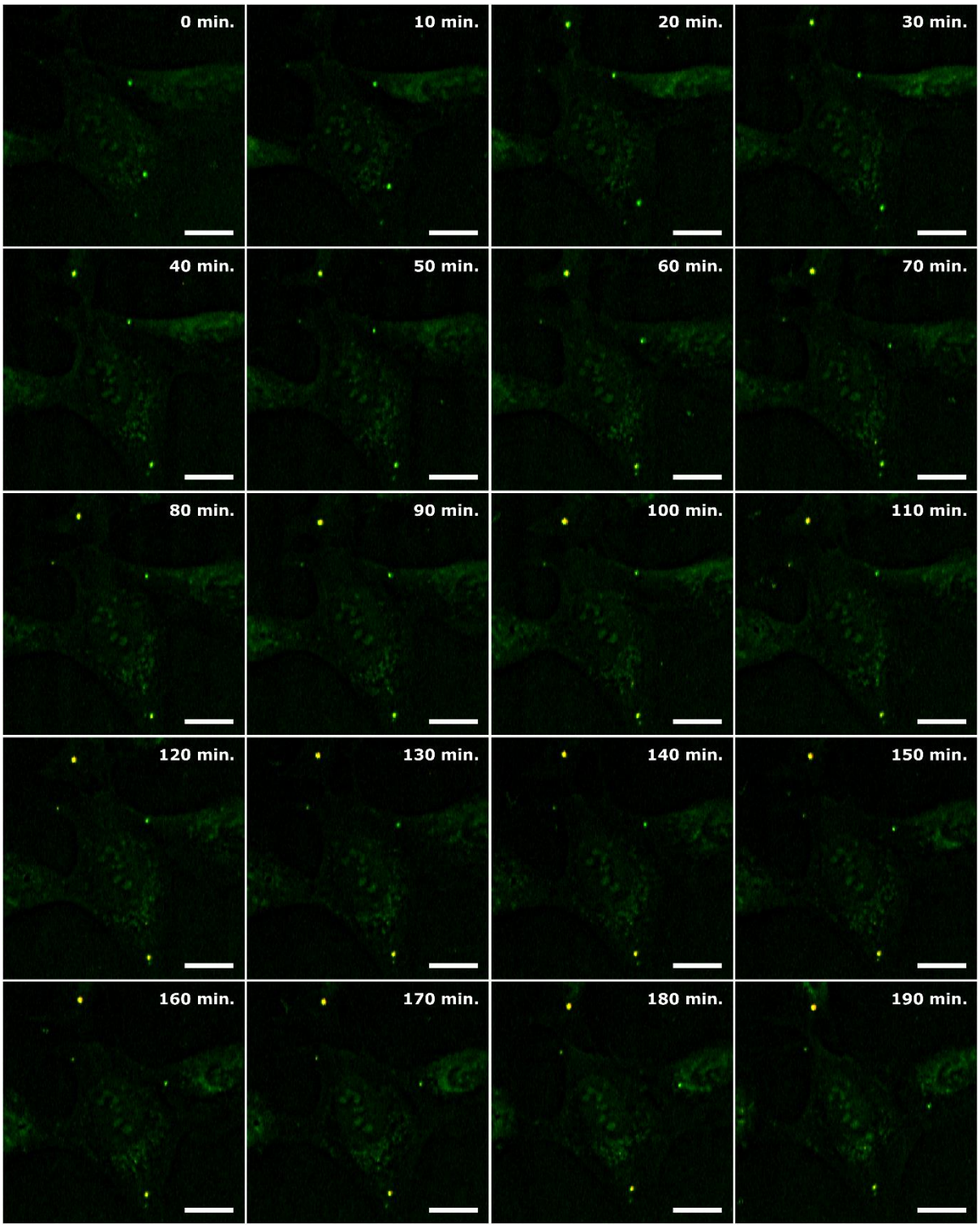

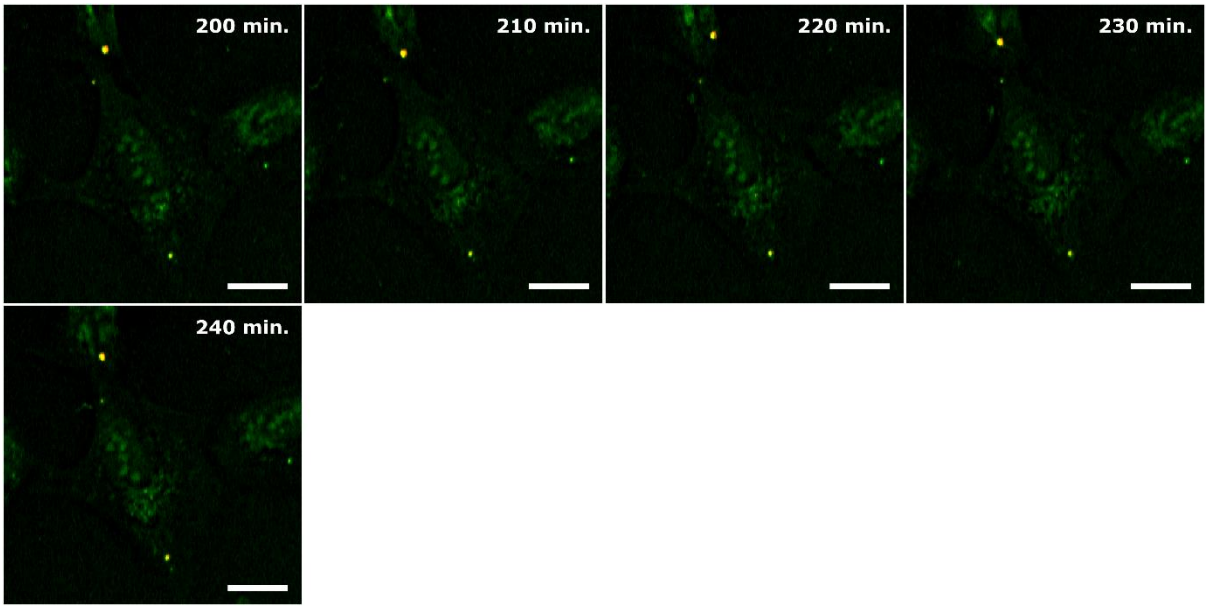

Figure S10. Time-lapse 2C-IP images of living U2OS cells exposed to 250 µM PA-d$_{31}$. The two-color IP images were obtained every 10 minutes for 4 hours. The color scheme is the same as in Figure S3A (red: 2,193 cm^{-1}, green: 2,855 cm^{-1}). Cutoff frequency, 70 Hz. Step size, 400 nm. Pixel dwell time, 2 ms. Probe power, 15 mW. IR excitation power, 0.2 mW (at 2,193 cm^{-1}) and 0.1 mW (at 2,855 cm^{-1}). Scale bars, 20 µm.

SupplementaryNote 11. Fixed U2OS specimen after time-lapse measurements

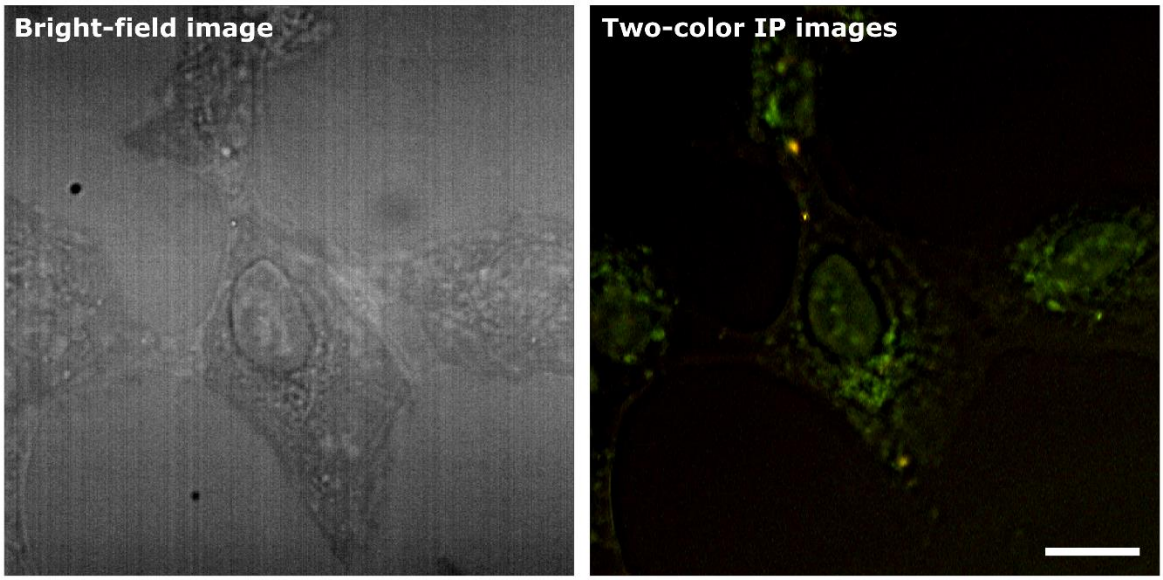

Figure S11. Bright-field and 2C-IP images of fixed U2OS specimen after time-lapse measurement. Cutoff frequency, 70 Hz. Step size, 200 nm. Pixel dwell time, 2 ms. Probe power, 15 mW. IR excitation power, 0.2 mW (at 2,193 cm^{-1}) and 0.1 mW (at 2,855 cm^{-1}). The color scheme is the same as in Figure S3A (red: 2,193 cm^{-1}, green: 2,855 cm^{-1}). Scale bars, 20 μm.

Supplementary Note 12. IP images for varying pixel dwell times

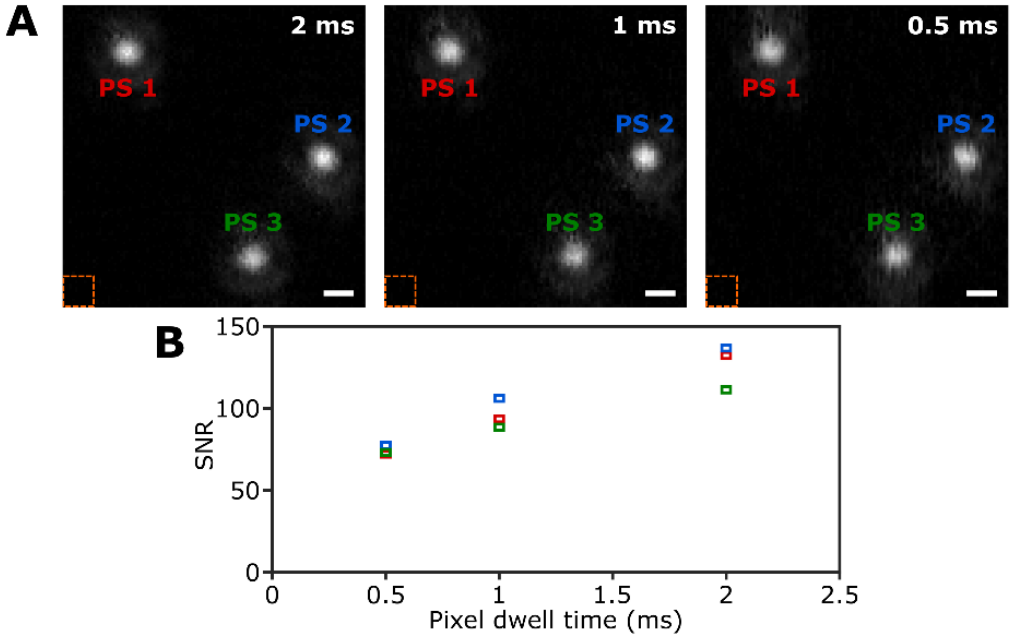

Figure S12. IP image and SNR of 1-µm polystyrene beads under different pixel dwell times. (**A**) IP images of 1 µm polystyrene beads at different pixel dwell times (2, 1, and 0.5 ms). Cutoff frequency, 280 Hz. Step size, 100 nm. Probe power, 15 mW. IR excitation power, 0.2 mW (2,850 cm^{-1} and 100 kHz) (**B**) Signal-to-noise ratio (SNR) of three polystyrene (PS) beads. The noise was obtained at the region indicated by the orange dotted box in the IP image, and the maximum signal of each PS bead was selected to calculate SNR. The SNR of 1 µm PS beads is estimated to be greater than 70, even with a pixel dwell time of 0.5 ms.